
Design of swashplate axial piston machines having low piston transverse forces

Mohamed Elashmawy^{1,2}

¹Mechanical Engineering Department, Engineering College, University of Hail, Hail, Saudi Arabia

²Engineering Science Department, Faculty of Petroleum and Mining Engineering, Suez University, Suez, Egypt

Email address:

arafat_696@yahoo.com

To cite this article:

Mohamed Elashmawy. Design of Swashplate Axial Piston Machines Having Low Piston Transverse Forces. *International Journal of Mechanical Engineering and Applications*. Special Issue: Advanced Fluid Power Sciences and Technology. Vol. 3, No. 1-2, 2015, pp. 17-23. doi: 10.11648/j.ijmea.s.2015030102.13

Abstract: Axial piston machine of swashplate type is the common design widely used for many hydraulic applications because of its simplicity, compact design and low cost. However, this simplicity has a negative effect for piston transverse forces which limits machine performance. The main target of this study is to investigate a feasible design of a fixed displacement swashplate contour in order to minimize piston transverse forces. The design should compensate the contact surface mechanism between swashplate and piston end. Piston slipper is replaced by a ball that is rotatably mounted within a ball socket formed at the piston end. The ball runs on a circumferential contour groove formed on the swashplate surface. The sliding friction between swashplate and slipper is replaced by a rolling friction between ball and circumferential runway groove. Primary results show a rough estimation of 30% reduction of piston transverse forces due to the cam action radial forces elimination. This reduction promises to enhance overall machine performance.

Keywords: Hydraulic, Swashplate, Axial Piston, Transverse Forces, Tribological Contact

1. Introduction

In an axial piston machines, the axes of the pistons are parallel to the axis of rotating cylinder block. A swashplate axial piston machine has a cylinder block which contains a number of cylinders. The cylinder block rotates taking the pistons with it. The end of each piston exposed to inclined swashplate. The stroke of the pistons depends on tilt angle of the swashplate. Controlling the tilt angle controls the displacement of the machine. The inlet and outlet ports are formed in a separate non-rotating plate (valve plate) mated to the surface of the rotating cylinder block. The suction port of the axial piston pump is exposed to the outward pistons while the delivery port is exposed to the inward pistons. This situation remains unchanged with rotation; the liquid always flows from the suction port to the delivery port. The opposite is true for the swashplate piston motors.

Due to the narrowness of the clearance of the tribological contact between piston-cylinder pair, sealing of the piston machines is very high compared to other oil machine types. The three main tribological contact friction pairs of swashplate axial piston machines (*piston-cylinder pair,*

swashplate-slipper pair and cylinder block-valve plate pair) have serious wearing problems at tribological contact areas which limit machine pressure and lifetime. Lubrication plays a key role in the design of such machines. The swashplate-slipper pair is subjected to the highest friction level due to tilt angle and transverse forces acting on the piston end. In case of very high pressure needs, a radial piston pump design should be used.

Great efforts were paid to reduce friction forces in the swashplate piston machines. The most concern was about the friction forces within piston-cylinder friction pair. A geometry study of the piston-cylinder contact, is optimized by comparing test bench results. Both, piston and cylinder are to be coated or should consist of hardened material. Results show that contouring and geometry can be optimized for specific working points [1].

Surface treatment of cylinder barrel coated by TiN plasma within axial piston pumps was used. Results show that the friction of the valve plate mated with a TiN-coated cylinder barrel could be reduced to 22% compared to uncoated one under 300 bar and 100 rpm rotational speed [2].

Numerous researches concerning the slipper-swashplate friction pair have been conducted. This parameter is quite

important because of its high effect on the friction force between piston and inner cylinder surface due to piston transverse forces. Increasing transverse forces will lead to an increase of piston and cylinder friction as well as a surfaces wearing. Static and dynamic characteristics of a piston pump slipper with a groove have been studied using 3-D Navier Stokes equation. The effect of different dimensions and position and rotational speed of grooves on pressure, leakage, torque and force were also simulated. Results show that when modifying groove position, moving the groove towards the slipper inner pocket increases leakage and force acting over the slipper, while when the groove is positioned near the outer boundary of the slipper, decreasing the groove width increases the force on the slipper and decreases the leakage [3].

A simulation model is developed for the dynamic micro-motion, the pressure distribution and leakage of the swashplate-slipper friction pair is included in the model. Results show that the oil film can be very thin in some positions due to slipper tilt causes a partial abrasion on the outer part of sealing belt. The partial abrasion will intensify the tilting degree of slipper and accelerate partial abrasion further which leads slipper leakage to increase. In order to improve the oil carrying ability of slipper and reduce the partial abrasion, the slope on the inner edge of sealing belt should be optimized. This will cause the efficiency of the pump to be improved due to slipper leakage reduction [4].

The major part of a model designed for axial piston machines is dedicated to the lubrication of the three main pump sliding interfaces, including slipper-swashplate pair, and considers the impact of elasto-hydrodynamic, thermal, and micro-motion effects on fluid film thickness. Simulation results are compared to measurements taken of a commercially manufactured pump interface. Development of more efficient slipper designs could be performed using this new insight [5]. A sophisticated numerical transient model, considering thermo-elastohydrodynamic lubrication, has been developed to predict lubrication performance of swashplate-slipper pair. Results show the importance of correctly considering transient deformation squeeze pressure effects in a thin film lubrication model of the slipper swashplate lubricating interface [6].

Reducing piston transverse forces by using a ball piston bearing for an axial piston machines was the focus of an old US patent in 1967 by North [7]. Fig. 1 illustrates the mechanism using a piston with its outer end, equipped with a spherical socket within which a metal ball is free to rotate. The ball is rolling on a circumferential groove runway formed on the surface of the swashplate cam member. There are two cams, of each substantially plane and inclined by an angle of 80° to the cylinder block axis. The ball is hydraulically balanced and little leakage is allowed through one or more very small hall that opens the displacement chamber (high pressure) to the ball socket area (low pressure). The cost of manufacturing such ball and socket is quite small. No springs were needed for pistons to asses them in their outward movement. Springs were omitted because this embodiment is particularly proposed for use as a motor and the applied

pressure will force the pistons to move outwardly. In the case of pumps springs would be necessary [7].

An invention by Spielvogel that was published by US patent in 2012 was aimed to improve the performance of swashplate axial piston hydraulic machines. The design is shorter in length and the radial piston forces component is totally eliminated. Fig. 2 shows a longitudinal section of a piston with a spherical head and its circumferential swashplate cam [8]. This concept is similar to the invention of North [7] that illustrated in Fig. 1.

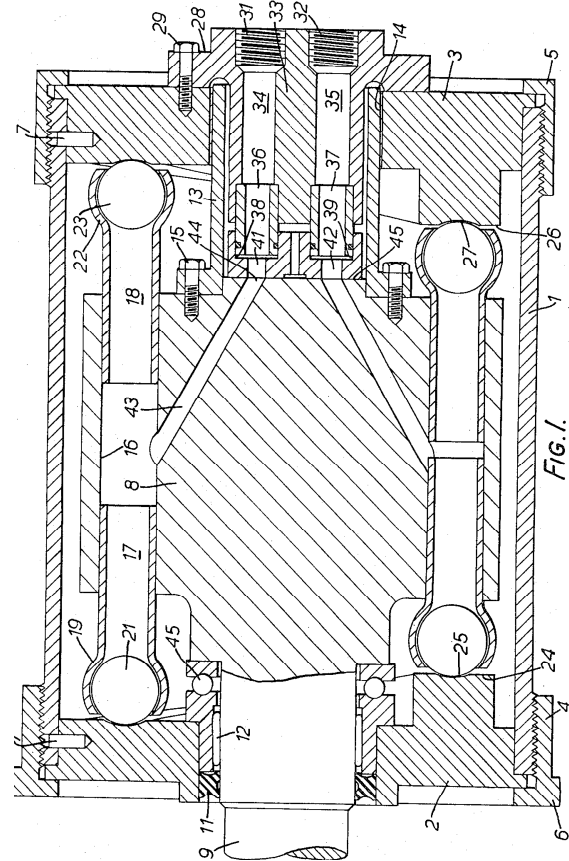


Figure 1. Cross-section through a hydraulic motor invention [7].

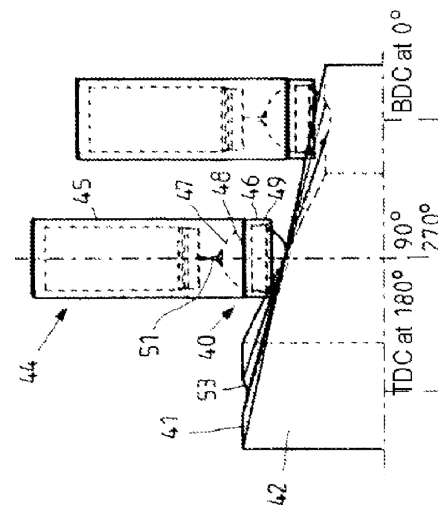


Figure 2. Cross-sectional view through a hydraulic motor invention [8].

2. Problem Statement

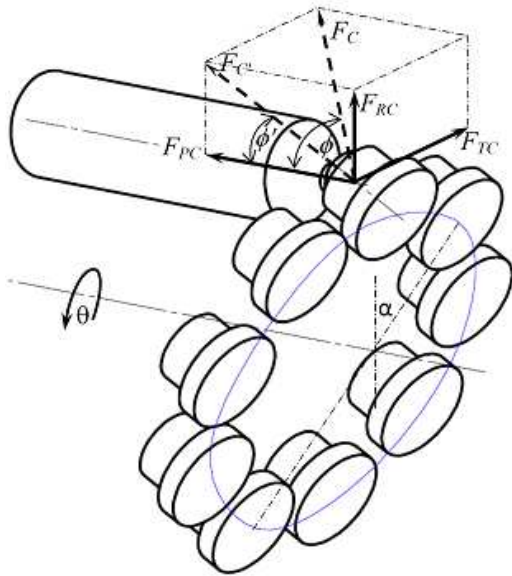


Figure 3. 3-D CAD showing the 9-piston slippers with the main angles and forces acting on the piston end.

The problem in focus of this study is to reduce piston transverse forces in the swashplate axial piston machines of fixed displacement type.

Working pressure of the swashplate axial piston machine is limited by piston transverse forces due to swashplate tilt angle (α) and friction forces caused by surface tribological contact between swashplate and slipper. As shown in Fig. 3 and Fig. 4a tilt angle (α) is directly affecting the cam action force (F_C). The cam action angle in the radial direction (ϕ') is unchanged for the current swashplate design and is equal to the tilt angle (α). Increasing α increases F_{RC} (cam action force in the radial direction). Increasing F_{RC} is at the expense of axial piston force (F_{PC}). Simply @ $\alpha=45^\circ \rightarrow \phi'=\alpha=45^\circ \rightarrow F_{RC}=F_{PC}$. Therefore, the tilt angle is limited and as a result the machine displacement is also limited.

3. Proposed Design

The main idea of the proposed design is to minimize the cam action angle (ϕ) under a condition of keeping the same pump displacement. Fig. 4, compares the geometry of the current swashplate design (Fig. 4a) with the geometry of the proposed circumferential cam contour design (Fig. 4b). The case selected is a piston at the *Outside Dead Center* (ODC) at the pump shaft rotational angle of $\theta=0^\circ$. This point is very clear as a starting point for comparison. In the current swashplate design, ϕ' is constant and equal to α . While in the proposed design, the cam action angle in radial direction (ϕ') is eliminated ($\phi'=0$) and consequently the cam action angle ϕ is reduced and varies from zero at $\theta=0^\circ$ to a maximum value at $\theta=90^\circ$. In comparison, the current design having ϕ varies from $\phi = \phi'$ at $\theta=0^\circ$ to a maximum value at $\theta=90^\circ$, see Fig. 12.

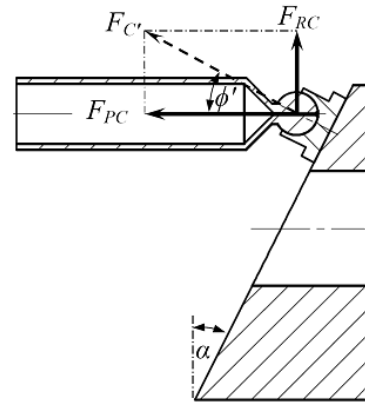


Figure 4a. Current swashplate design at ODC ($\theta=0^\circ$).

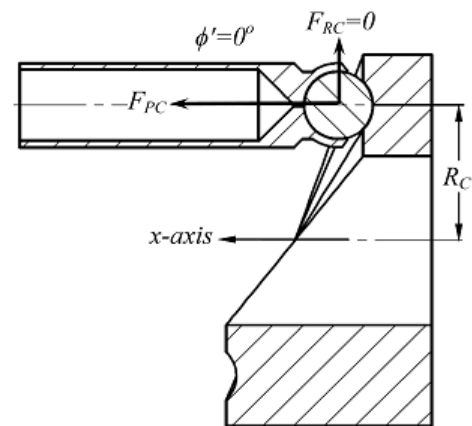


Figure 4b. Proposed circumferential cam contour design at ODC ($\theta=0^\circ$).

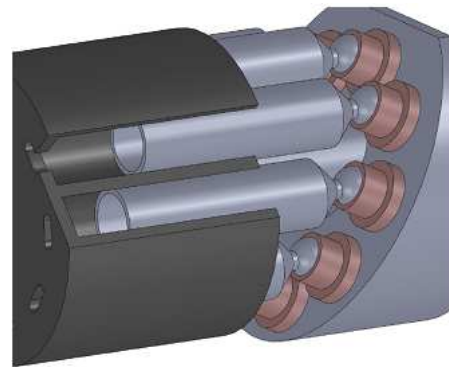


Figure 5a. Current swashplate design, 3D-CAD assembly.

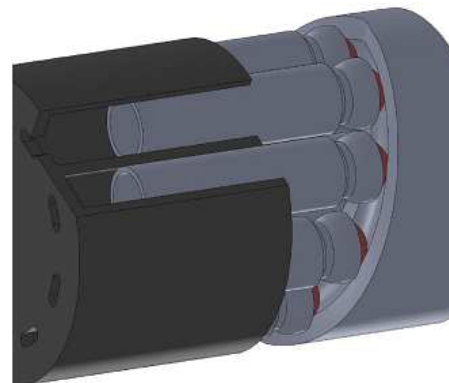


Figure 5b. Proposed design, 3D-CAD assembly.

Fig. 5 shows a 3 D-CAD mechanism comparison between the current swashplate design and the proposed circumferential cam contour design.

Fig. 6 shows 3 D-CAD mechanism comparison between the current swashplate design and the proposed design for one piston focusing on the relation between the piston end and the runway for each design. Figs. 5 and 6 show the ball and socket assembly replacing the slipper shoe mechanism and the circular runway of the ball bearing attached to the piston end.

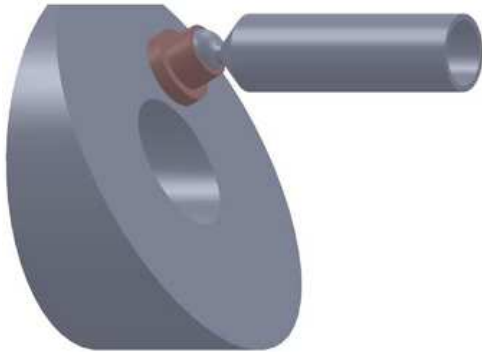


Figure 6a. Current swashplate design, 3D-CAD one piston assembly.

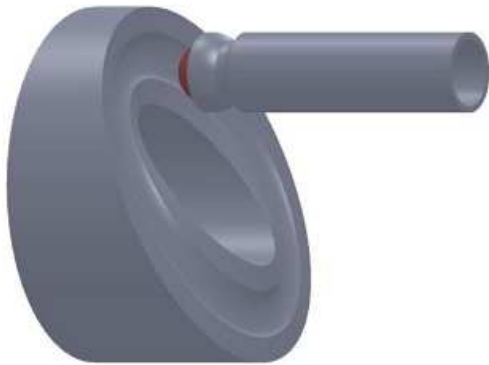


Figure 6b. Proposed circumferential cam contour design, 3D-CAD one piston assembly.

4. Results and Discussion

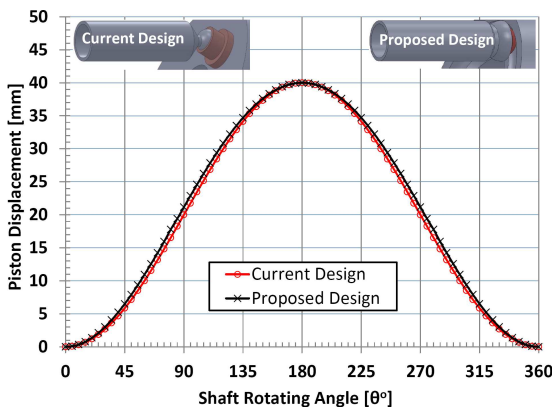


Figure 7. Comparison between piston displacement of current and proposed design, 3D-CAD geometry analysis.

Fig.7 shows the displacement of the piston in the current design in comparison with the displacement of the piston in

the proposed design. The displacement is measured using a 3D-CAD software (SolidWorks) based on the geometry analysis. This is done by rotating the pump shaft by 5° step angels and measuring the piston’s displacement using the measuring tool facility of the SolidWorks. The comparison between the two curves shows very small difference caused by the shifting of the ball and runway tangential contact position as shown in Fig. 10. This difference will be overlooked in this study.

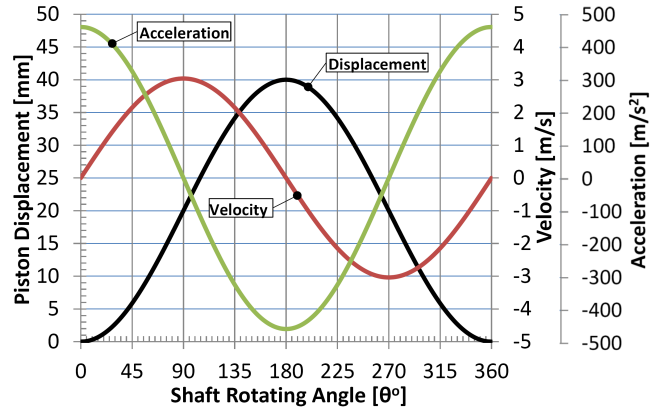


Figure 8. Displacement, velocity and acceleration of the proposed design, using Eqs. 1, 2 and 3.

The velocity and acceleration curves are considered as identical for both designs. Fig. 8 shows the displacement, velocity and acceleration for current design (also applicable for proposed design). Fig. 7 illustrates how the proposed design has no significant impact on the displacement, velocity or acceleration of the pump. Eqs. (1) - (3) describe the piston motion under swashplate cam action.

$$S_x = R_c \tan \alpha (1 - \cos \theta) \tag{1}$$

Knowing that $\theta = \omega t$ and deriving Eq.1 by time yields

$$v_x = \omega R_c \tan \alpha \sin \theta, \quad \omega = 2\pi N/60 \tag{2}$$

$$a_x = dv_x/dt = \omega^2 R_c \tan \alpha \cos \theta \tag{3}$$

Where: $N=1450 \text{ rpm}$, $\alpha = 26.57^\circ$ and $R_c=40\text{mm}$ were used as a case study for curves plotted in Fig. 8. In the present work, only a 3D-CAD model was built for both the current and the proposed designs, and all measurements were performed based on the geometry analysis. Therefore, the measurement of the cam action angle (ϕ) was used as the basis for the comparison. The transverse force acting on the end of the piston of the current design is affected by the following parameters:

- Piston end and slipper centrifugal forces acting on the radial direction Eq. 4.

$$F_{\omega G} = m_G R_C \omega^2 \tag{4}$$

- Friction between slipper and cam surface
- The cam action force which strongly depends on the swashplate tilt angle.

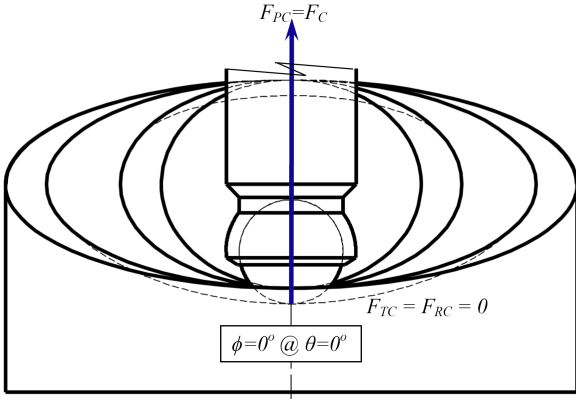


Figure 9. Cam action angle at ODC, ($\phi=0^\circ$ at $\theta=0^\circ$).

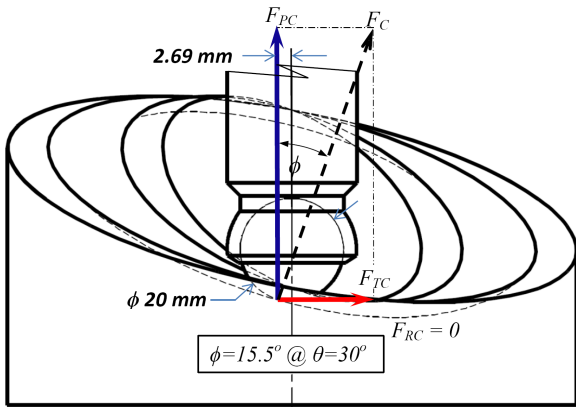


Figure 10. Cam action angle at 30° from ODC, ($\phi=15.5^\circ$ at $\theta=30^\circ$).

The proposed design has the potential to eliminate the transverse force due to cam action in radial direction (F_{RC}). In addition it also reducing the slipper friction force by replacing slipping friction (current design) by a ball bearing rolling friction (proposed design). This will lead to an overall reduction in the total transverse forces acting on the piston end (F_T). Figs. 9 and 10 show the measurements of the cam action angle (ϕ) using the 3D geometry assembly design. Starting with ODC $\phi=0^\circ$ at $\theta=0^\circ$, Fig. 9. Then ϕ is measured for each 5° step of the shaft angle (θ). Fig. 10 shows the cam action angle ($\phi=15.5^\circ$) at $\theta=30^\circ$. Fig. 10 shows the dashed curve tangent to the ball surface which represents the cam contour formed in the swashplate. The contact tangent point between the dashed curve and the ball circle (20 mm) is slightly shifted to the left by 2.69 mm. This shift produces torque on the piston due to non-axial force pushing the piston (F_{PC}).

The maximum possible cam action angle (ϕ) measured for the proposed design was almost equal to the swashplate tilt angle and was at $\theta=90^\circ$, ($\phi_{max}=26.3^\circ$), Fig. 11. At $\theta=90^\circ$, the contact tangent point shift was also the maximum and measured as 4.52 mm. The analysis of the forces acting on the piston end is illustrated in Fig. 11. The radial direction is perpendicular to the paper plane direction and the total transverse force (F_T) acting on the piston end is shown in details in the right hand side of Fig. 11 and enclosed inside a box. The centrifugal force ($F_{\omega G}$) could be calculated by Eq. 4. The centrifugal force is assumed to be roughly the same for both designs. The most important and effective component is

the friction force between cam and piston end. This component is beyond the scope of this study, but it was most likely reduced by the ball bearing rolling friction achieved by the proposed design.

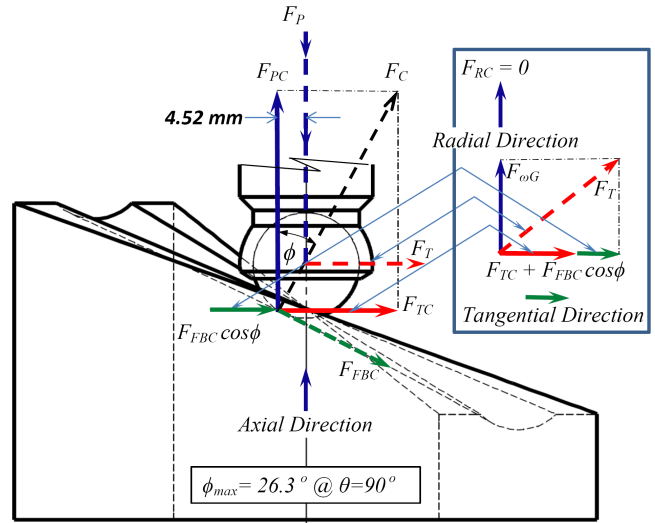


Figure 11. Cam action angle ($\phi_{max}=26.3^\circ$ at $\theta=90^\circ$).

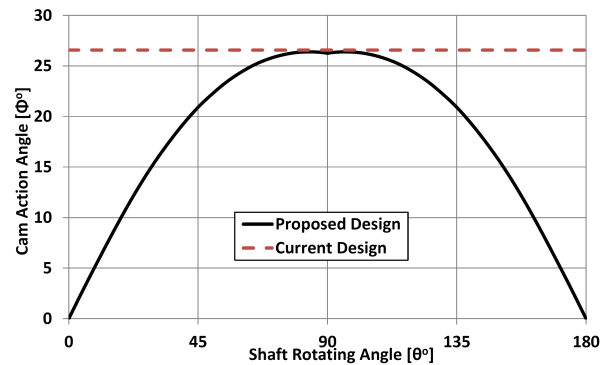


Figure 12. Comparison between came action angle (ϕ) for current swashplate design and proposed design.

Fig. 12 shows a comparison between the measured cam action angle (ϕ) for the current and the proposed designs as a function of the shaft rotating angle (θ). The relation between the transverse force and the cam action angle (ϕ) is derived according to the force analysis illustrated in Fig. 11 and can be explained as follows:

$$F_{TC} = F_C \sin \phi \tag{5}$$

Force balance at piston axial direction yields:

$$\sum F_{axial} = 0$$

$$F_{PC} = F_P = F_C \cos \phi \rightarrow F_C = F_P / \cos \phi \tag{6}$$

Piston force is mainly related to the pump working pressure $F_P = P A_p$. substituting in Eq. 5 yields:

$$F_{TC} = P A_p \tan \phi \tag{7}$$

Eq. 7 is plotted on Fig. 13 to compare the current and the proposed designs.

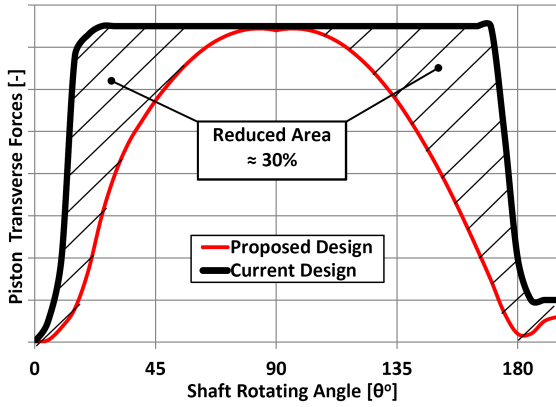


Figure 13. Comparison between current and proposed designs concerning transverse force and expected power reduction during delivery stroke.

Fig. 13 compares the transverse forces of the current and the proposed designs. This curve is based on a rough estimation and states an expected 30% reduction of the transverse forces.

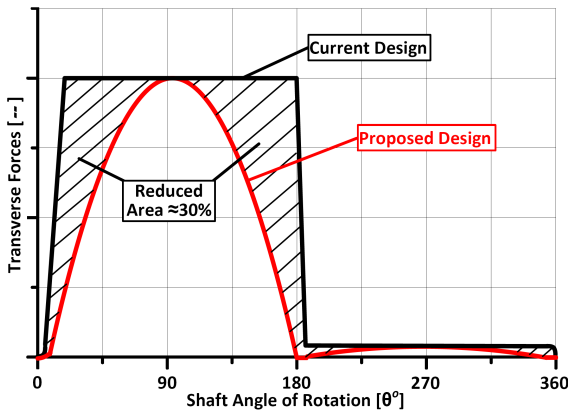


Figure 14. Comparison between current and proposed designs concerning transverse force and expected power reduction during delivery and suction strokes ($\theta=0^\circ$ to $\theta=360^\circ$).

Fig. 14 shows a comparison between the transverse forces of the current and the proposed designs for complete shaft rotation. The comparison shows that transverse forces is maximum at delivery stroke ($\theta=0^\circ-180^\circ$) and minimum at suction stroke ($\theta=180^\circ-360^\circ$). Further experimental and theoretical investigations should be performed to determine the real and exact amount of reduction.

5. Conclusions

The proposed design holds the potential to reduce the transverse forces exerted on the piston for the fixed displacement swashplate piston machines. The expected power reduction is about 30% based on rough estimation and needs further investigations for accurate reduction evaluation. The proposed design will replace the sliding friction between swashplate and slipper by rolling friction between circumferential cam contour and ball bearing rotatably mounted at the piston outer end. These advantages are only limited to the fixed displacement swashplate piston machines due to geometry constraints. The proposed design needs

accurate machining processes and tolerance care for the circumferential cam contour manufacturing. At the same time the manufacturing process for the piston end will be more simpler than the current design of the sliding shoe. The piston end spherical socket and the ball are both common for manufacturing that are widely used for ball bearings applications. The proposed design is expected to reduce machine power consumption and increase its efficiency and life time. In case of motor applications, no springs are needed for pistons to assess them in their outward movement. The applied pressure will force the pistons to move outwardly. While for pumps springs would be necessary.

It is highly recommended to perform an experimental investigation comparing the proposed design with an identical current swashplate design. Pressure limitation of the proposed ball bearing design should be also experimentally further investigated.

Acknowledgments

This study was supported and funded by the scientific research deanship, University of Hail (UoH), Hail, Saudi Arabia.

Nomenclature

α	Swashplate tilt angle	[deg]
θ	Shaft angle	[deg]
ϕ	Angle between F_{PC} and F_C	[deg]
ϕ'	Angle between F_{PC} and F_{RC}	[deg]
R_c	Radius of piston pitch circle	[mm]
ω	Angular velocity	[rad/s]
N	Rotational speed	[rpm]
S_x	Displacement in x-axis direction	[mm]
v_x	Velocity in x-axis direction	[m/s]
a_x	Acceleration in x-axis direction	[m/s ²]
F_C	Cam action force	[N]
F_P	Piston axial force	[N]
F_{PC}	Piston force, cam component	[N]
F_T	Piston transverse force, total	[N]
F_{TC}	Cam action force, tangential	[N]
F_{RC}	Cam action force, radial	[N]
F_{FBC}	Cam ball friction force	[N]
$F_{\omega G}$	Piston end centrifugal force, radial	[N]
m_G	Piston end and ball weight	[kg]
A_P	Piston cross sectional area	[m ²]
P	Working pressure	[bar]
<i>Abbreviations</i>		
ODC	Outer Dead Center	[$\theta=0^\circ$]
IDC	Inner Dead Center	[$\theta=180^\circ$]

References

- [1] S. Gels and H. Murrenhoff, Simulation of the lubricating film between contoured piston and cylinder, *International Journal of Fluid Power IJFP*, Vol. 11, No. 2 (2010) 15-24.

- [2] Y. Hong et al., Improvement of the low-speed friction characteristics of a hydraulic piston pump by PVD-coating of TiN, *Journal of Mechanical Science and Technology (KSME Int. J.)*, Vol. 20 No. 3, (2006) 358-365.
- [3] S. Kumar et al., Axial piston pump grooved slipper analysis by CFD simulation of three-dimensional NVE equation in cylindrical coordinates, *Elsevier, Computers & Fluids*, 38, (2009) 648-663.
- [4] Xu B, Zhang J H and YANG HuaY, Investigation on structural optimization of anti-overturning slipper of axial piston pump, *Sci China Tech Sci*, 55, (2012) 3010-3018, doi: 10.1007/s11431-012-4955-x.
- [5] A. Schenk, M. Zecchi, and M. Ivantysynova, Accurate Prediction of Axial Piston Machine Performance Through a Thermoelastohydrodynamic Simulation Model, *In: ASME Symp. FPMC (2013)* 2013-4456.
- [6] A. Schenk and M. Ivantysynova, A transient fluid structure interaction model for lubrication between the slipper and swashplate in axial piston machines, *The 9th International Fluid Power Conference, 9. IFK, March 24-26, Aachen, Germany*, (2014).
- [7] John D. North, Reciprocating pistons for pumps and motors, *United States Patent Office, US 3356037A*, (1967).
- [8] Christian Spielvogel, Axial piston machines having a swashplate design. *United States Patent Office, US 2012/0279387 A1*, (2012).